Acta Biomaterialia 180 (2024) 128–139

Contents lists available at ScienceDirect

Acta Biomaterialia

journal homepage: www.elsevier.com/locate/actbio

Full length article

Inflammatory tissue response in human soft tissue is caused by a higher particle load near carbon fiber-reinforced PEEK compared to titanium plates

E Fleischhacker[a,*], CM Sprecher[b], S Milz[c], MM Saller[a], R Wirz[d], R Zboray[e], A Parrilli[e], J Gleich[a], G Siebenbürger[a], W Böcker[a], B Ockert[a], T Helfen[a]

[a] Department of Orthopedics and Trauma Surgery, Musculoskeletal University Center Munich (MUM), LMU University Hospital, LMU Munich, Germany
[b] AO Research Institute Davos, Clavadelerstrasse 8, 7270 Davos, Switzerland
[c] Anatomische Anstalt der Ludwig-Maximilians-Universität, Pettenkoferstrasse 11, 80336 München, Germany
[d] RMS Foundation, Bischmattstrasse 12, 2544, Bettlach, Switzerland
[e] EMPA, Überlandstrasse 129, Dübendorf, Switzerland

ARTICLE INFO

Article history:
Received 28 November 2023
Revised 19 March 2024
Accepted 11 April 2024
Available online 16 April 2024

Keywords:
CFR-PEEK
Particle release
Titanium
Foreign body reaction
Peri-implant tissue inflammation
Plate osteosynthesis

ABSTRACT

Titanium as the leading implant material in locked plating is challenged by polymers such as carbon fiber-reinforced polyetheretherketone (CFR-PEEK), which became the focus of interest of researchers and manufacturers in recent years. However, data on human tissue response to these new implant materials are rare.

Osteosynthesis plates and peri–implant soft tissue samples of 16 healed proximal humerus fractures were examined (n = 8 CFR-PEEK, n = 8 titanium). Soft tissue was analyzed by immunohistochemistry and µCT. The entrapped foreign bodies were further examined for their material composition by FTIR. To gain insight into their origin and formation mechanism, explanted and new plates were evaluated by SEM, EDX, profilometry and HR-CT.

In the peri–implant soft tissue of the CFR-PEEK plates, an inflammatory tissue reaction was detected. Tissues contained foreign bodies, which could be identified as tantalum wires, carbon fiber fragments and PEEK particles. Titanium particles were also found in the peri–implant soft tissue of the titanium plates but showed a less intense surrounding tissue inflammation in immunohistochemistry. The surface of explanted CFR-PEEK plates was rougher and showed exposed and broken carbon fibers as well as protruding and deformed tantalum wires, especially in used screw holes, whereas scratches were identified on the titanium plate surfaces.

Particles were present in the peri–implant soft tissue neighboring both implant materials and could be clearly assigned to the plate material. Particles from both plate materials caused detectable tissue inflammation, with more inflammatory cells found in soft tissue over CFR-PEEK plates than over titanium plates.

Statement of significance

Osteosynthesis plates are ubiquitously used in various medical specialties for the reconstruction of bone fractures and defects and are therefore indispensable for trauma surgeons, ENT specialists and many others. The leading implant material are metals such as titanium, but recently implants made of polymers such as carbon fiber-reinforced polyetheretherketone (CFR-PEEK) have become increasingly popular. However, little is known about human tissue reaction and particle generation related to these new implant types. To clarify this question, 16 osteosynthesis plates (n = 8 titanium and n = 8 CFR-PEEK) and the overlying soft tissue were analyzed regarding particle occurrence and tissue inflammation. Tissue inflammation is clinically relevant for the development of scar tissue, which is discussed to cause movement restrictions and thus contributes significantly to patient outcome.

* Corresponding author.
E-mail address: evi.fleischhacker@med.uni-muenchen.de (E. Fleischhacker).

https://doi.org/10.1016/j.actbio.2024.04.023
1742-7061/

1. Introduction

Dislocated fractures of the human skeleton can be treated by open reduction and locked plating, using anatomically pre-shaped plates [1–3]. These plates are available in a variety of implant materials, which have attracted increasing attention in recent years. In addition to stainless steel, titanium and its alloys have been established as a standard implant material [4]. Titanium is inert, has a comparable elasticity to cortical bone and contains no nickel or chromium, which both can lead to allergic reactions, particularly in contrast to stainless steel. Yet, stainless steel previously dominated the market for decades [4,5]. However, surgical grade stainless steel consists largely of nickel and the number of people suffering from hypersensitivity to that transition metal has increased significantly over the years, so that steel has come under criticism, which helped titanium alloy to a buoyant rise [4]. In 2003, Voggenreiter et al. published a study in which they investigated the immune-inflammatory tissue response to steel and titanium implants in vivo [5]. They found a significantly increased number of inflammatory cells in soft tissue over steel as well as in tissue over titanium plates [5]. A different study showed a significant amount of particle release in tissue around titanium implants in mini pig maxillae [6]. Furthermore, the authors found increased cytotoxicity and DNA damage caused by titanium particles, compared to equally sized zirconium ceramic particles [6]. This shows that titanium is not an ideal implant material either, even if it does not lead to allergic reactions. So, researchers and manufacturers are still looking for an optimal solution. A fairly new implant material is carbon fiber-reinforced polyetheretherketone (CFR-PEEK) [7]. In contrast to metallic implants, the thermoplastic polymer is biocompatible, non-allergenic and non-mutagenic, heat-resistant, corrosion-free, and radiolucent [7,8]. The materials hydrophobic properties are seen as a reason for fewer adhesion to surrounding tissues [9]. However, a study published in 2019 showed that in animal experiments with mini-pigs significantly more multinuclear giant cells were present in the soft tissue over dental implants made of CFR-PEEK, compared to the soft tissue over titanium caps [10]. Moreover, it remains unclear how the human organism reacts to CFR-PEEK particles of varying sizes. Evaluations of humane tissue are rare. The authors only found case descriptions but no publication in which the reaction of the human organism to CFR-PEEK implants has been investigated systematically, especially with respect to longer-term implantation of mechanically loaded osteosynthesis plates [11–13]. In 2016 Merolli et al. described the case of a woman that suffered from destructive tenosynovitis after open reduction and internal fixation (ORIF) of a distal radius fracture with a CFR-PEEK plate. In the histopathological examination they found a granulomatous reaction with multi-nucleated giant cells and carbon fibers within fibrous tissue [13].

In the present study a systematic histological evaluation of the peri–implant soft tissue after open reduction and locked plating with CFR-PEEK and titanium plates of proximal humerus fractures was obtained. Particle analysis of enclosed and free foreign bodies, their interaction with the surrounding soft tissue and the analysis of the plates themselves allowed to gain further insights into the origin and biological relevance of the foreign bodies.

2. Materials and methods

After approval of the retrospective study design by the Local Ethics Committee of the Ludwig-Maximilians-University (LMU) Munich, Germany, the study was conducted in accordance with CONSORT (CONsolidated Standards of Reporting Trials) 2010 policy and the Helsinki Declaration. All patients agreed to participate in this study with written detailed informed consent.

The study included 16 patients who were treated by open reduction and locked plating for a proximal humerus fracture either with an implant made of CFR-PEEK or titanium and suffered of impaired movement and/or persistent pain after fracture healing, which is why the indication for implant removal was given. Each group (CFR-PEEK vs. titanium) consisted of $n = 8$ patients. All operations were performed via a delto-pectoral approach. Between the primary fracture treatment and implant removal, none of the patients underwent surgery on the affected shoulder.

2.1. Implants

The CFR-PEEK plate used in this study was the PEEKPower® humeral fracture plate (Arthrex, Naples, Florida, USA) (see Fig. 1A–C). This anatomically pre-shaped plate consists of CFR-PEEK, in which radio dense tantalum wires are embedded (Fig. 1B and b). For fixation to the bone, titanium-aluminum-vanadium alloy (according to ISO 5832-3) screws are used, which can be fixed polyaxially and locked in the plate. Therefore, a thread is cut into the bushing by the screw heads themselves, allowing polyaxially locked plating (Fig. 1c). This provides fixation of the screws in areas with better bone quality, which is of particular advantage in patients with reduced bone mass density.

The titanium alloy implant for osteosynthesis of proximal humerus fractures used in this study was the PHILOS® (DePuy Synthes, Johnson & Johnson Medical, Raynham, Massachusetts, USA), an anatomically pre-shaped plate with pre-manufactured holes and milled threads, in order to allow monoaxial locking of titanium screws and to realize the principle of angular stability (see Fig. 1D–F).

2.2. Patient collective, tissue and implant collection

The decision as to which implant was used in the patients was made by the surgeon at the time of fracture treatment and thus before the initiation of this retrospective study. The mean age of the participants was 53.9 ± 15.5 years (mean ± standard deviation; CFR-PEEK 58.6 ± 17.5 vs. titanium 49.3 ± 12.6; $p = 0.279$ Mann Whitney test). After radiologically confirmed fracture healing, the implants were removed through the same delto-pectoral approach used for fixation. Criteria for exclusion were misplaced implant, healing in malposition, implant breakage, infection, avascular necrosis, concomitant pathology requiring therapy and age less than 18 years. No deviations in radiologically confirmed fracture healing were observed between study groups.

The reasons for implant removal were persistent pain and/or limitation of movement. Implant removal occurred on average 13.7 ± 5.8 months (mean ± standard deviation; CFR-PEEK 11.6 ± 2.8 vs. titanium 15.9 ± 7.4; $p = 0.279$ Mann Whitney test) after fracture treatment. After skin incision and preparation through the muscles, the soft tissue layer (Fig. 2[A] and [B]) lying over the plate was prepared thoroughly, removed and parts of it frozen at −20 °C for further processing. Finally, most of the material was used for routine paraffin histology.

2.3. µCT of peri–implant soft tissue

For localization and non-destructive mapping of possibly entrapped particles within the peri–implant soft tissue, µCT-scans with a custom build research CT (CT-alpha, ProCon X-Ray, Sarstedt, Germany) were performed. The CT scanner was equipped with a nano focus X-ray source (XWT-225-TCHE, X Ray Worx, Germany) and a 75 µm pixel size CMOS flat panel detector (Dexela 2923, PerkinElmer, USA) at a 2 × 2 binning. Soft tissue samples were immersed in 70 % ethanol and placed in a closed 35 mm dish, which

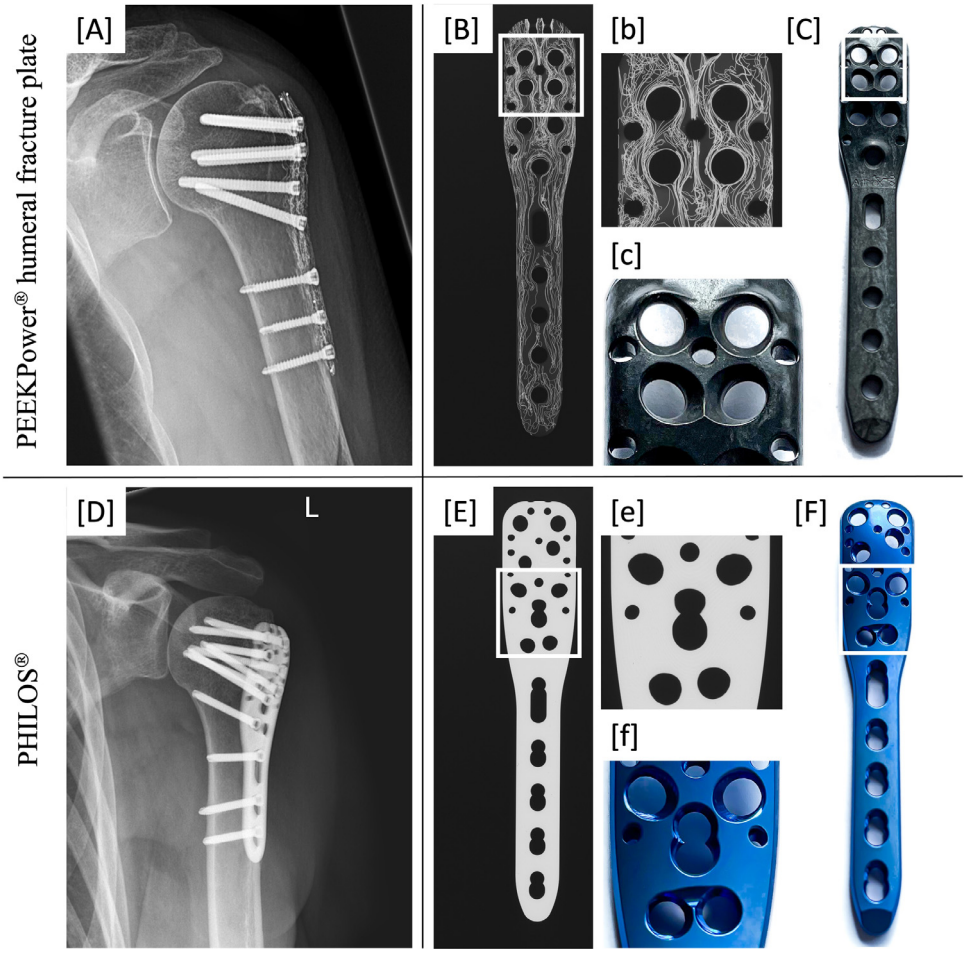

Fig. 1. [A]–[C] and [D]–[F] show radiographs and photographs of the plates used. [b] and [c] as well as [e] and [f] show the different hole configurations: While the CFR-PEEK (PEEKPower® humeral fracture plate) plate holes are not threaded (see [c]) until the screws are inserted, the threads in the titanium plates (PHILOS®) are pre-milled (see [f]). The bright white tantalum wires in CFR-PEEK plate were visible in the X-ray of the patient [A] as well as in the images of the plate without any tissue [B, b].

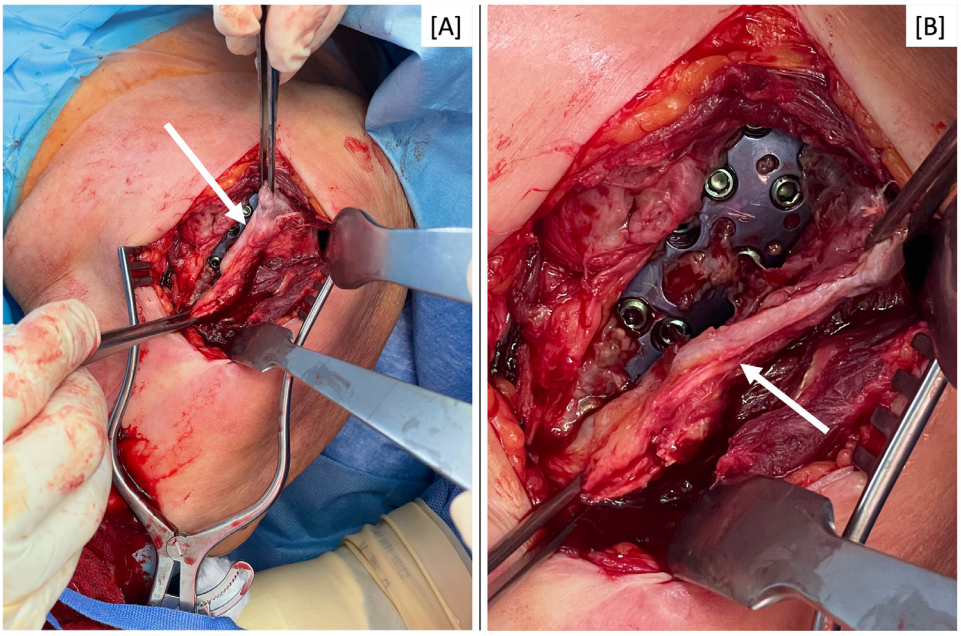

Fig. 2. Intraoperative views of a plate with the overlying soft tissue (white arrows) which is removed for further examination after detachment from the underlying titanium plate.

was mounted on a custom designed 3D-printed samples holder. Scan parameters are shown in Suppl. Tab. 1.

Acquired raw data was reconstructed with X-Aid (version 2020.10.1, MITOS GmbH, Garching, Germany) after correction for geometrical errors and beam hardening. The evaluation was performed in Dragonfly Pro (ORS, Montreal, Quebec, Canada).

2.4. Histology

Paraffin-embedded sections were deparaffinized in xylene and then rehydrated in descending series of alcohol. Standard Haematoxylin Eosin stained sections were prepared prior to the immunohistochemical investigation. For immunohistochemical detection of macrophage and inflammation associated antigens, sections were first blocked with Vector Labs "Bloxall" (SP6000) followed by a treatment with 5 % horse serum diluted with phosphate buffered saline solution (PBS). Incubation with the primary antibodies was performed overnight in a moist chamber at 4 °C. A panel of monoclonal antibodies against CD68, CD163, mature, tissue fixed macrophage antigen and calprotectin was used to identify and localize macrophages of different, inflammation related phenotypes (Suppl. Tab. 2). Sections were then washed with PBS and incubated with a biotinylated horse anti-mouse secondary antibody (Vector Labs, Newark, CA, USA) for 30 min at room temperature. After another washing step with PBS an earlier prepared ABC-Complex was applied for 30 min at room temperature. Then, after additional washing steps with PBS a 4 min incubation in the dark with Vector Impact DAB substrate (Vector Labs, Newark, CA, USA) followed. After a washing step in tap water, counter staining was performed with Meyer's haematoxylin (Sigma-Aldrich CAS 517-28-2, Germany). For negative control, the primary antibody was replaced with PBS. The immunohistochemical analysis was based on a semi-quantitative assessment score and was counting positive cells per tissue section (no cells positive (0), one cell positive ((+)), 2 or more cells, but less than 10 (+), 10 or more cells positive (++)).

2.5. Infrared microscopy (FTIR)

In order to examine the particles in the soft tissue more precisely with regard to their material composition, peri–implant tissue samples were embedded in PMMA, stained with Giemsa-eosin stain and underwent Fourier transform infrared spectroscopy (FTIR) analysis without further sample preparation. The samples were placed under the FTIR microscope (LUMOS FTIR microscope, Bruker, Germany), and various locations across the samples were analyzed using the attenuated total reflectance (ATR) method. The germanium ATR crystal (tip diameter about 100 µm) was brought into contact with the sample surface, and depending on the size of the particles, infrared spectra with an area of 10×10 µm^2 to 36×36 µm^2 were evaluated. The area of a target spot was defined by the variable aperture inside of the instrument. With this technique, infrared light can detect information down to a penetration depth of about 0.2–1.1 µm in the sample.

2.6. High resolution CT-scans of paraffin-embedded soft tissue and plates

For further characterization of the particles in the soft tissue and to identify the localization on the plates from which these particles originated, high-resolution (HR-) CT-scans of the paraffin-embedded tissue samples and plate samples were performed using the RX Solutions EasyTom XL system (RX Solutions, Chavanod, France). This was done by cutting cubes of approximately $35 \times 9 \times 10$ mm out of the explanted plates. Similarly, cubes of approximately $9 \times 9 \times 9$ mm were excised from the paraffin-embedded soft tissue specimens. The choice was made for regions that indicated a relevant particle load in CT scans of the peri–implant soft tissue. The scan parameters for investigation of different aspects of the CFR-PEEK plates and of the paraffin-embedded tissue samples are summarized in Suppl. Tab. 1. The scan parameters have been optimized to the different objectives of the examination. Different combination of two micro-focus tubes and two detector types were used depending on the objectives. These are: a 230 kV reflection type micro-focus and a 100 kV transmission-type nano-focus X-ray tube both from Hamamatsu; a Varian PaxScan 2520DX flat panel detector (with a columnar CsI converter; 1920×1536 pixel matrix; pixel pitch of 127 μm; 16 bits of dynamic range) and a high-resolution CCD camera (Ximea) coupled to a 20 μm-thick Gadox scintillator through optical fibers with a detection matrix of 2016×1344 pixels and an effective pixel size of 18 µm. For soft materials at high resolution (CFR-PEEK plate and soft tissue sample), the X-ray propagation-based phase contrast technique was utilized to improve the contrast-to-noise ratio of the images. For phase retrieval, the well-known Paganin method [14] was used under the assumption of single-material object. As common practice for broad-spectrum laboratory sources, the parameters of the Paganin filter, in this case specifically the −6 dB cut-off frequency, is tuned manually by visual inspection of the image and was set to around 3.5 % of the Nyquist frequency [15]. After phase retrieval, for the 3D reconstruction filtered back projection by the FDK algorithm [16] in the commercial software Xact of RX Solutions was used just as for all the other HR-CT-scans.

2.7. Scanning electron microscopy and energy dispersive X-ray analysis

To identify the areas on the plates from which the particles originate and to differentiate what material they are of, the scanning electron microscopy (SEM) imaging were done with the Scanning electron Microscope (SEM, S-4700 II FESEM, Hitachi High Technologies, Tokyo, Japan). For this purpose, all samples were coated with a 20 nm thick carbon layer. Energy Dispersive X-ray analysis (EDX, Oxford Instruments, Abingdon, United Kingdom) was performed for elemental analysis.

2.8. Roughness measurement of surfaces by white light profilometry

The roughness measurement was done with uncleaned and used implants as well as new plates. Quantitative measurements were taken using a non-contact white light FRT MicroProf® 200 Profilometer equipped with a CWL 300 µm sensor (Fries Research & Technology, Germany) on $n = 6$ measurement points. The machining marks were oriented along the x-axis. The roughness value Ra (arithmetic average of the absolute values of the profile) was expressed in micrometers [17]. The calculations were performed on 1.0×1.0 mm scan areas with a point density of 1000 points/line along the x- and y-axis.

2.9. Statistics

Statistical analysis was performed using SPSS Statistics software, version 28 (IBM Corp. Released 2021. Amonk, NY, USA). Data are reported as mean ± standard deviation, for categorical data as absolute frequency with percentage distribution. The statistical analysis was done using a Mann-Whitney test for non-normally distributed values. The significance level was set at $p < 0.05$.

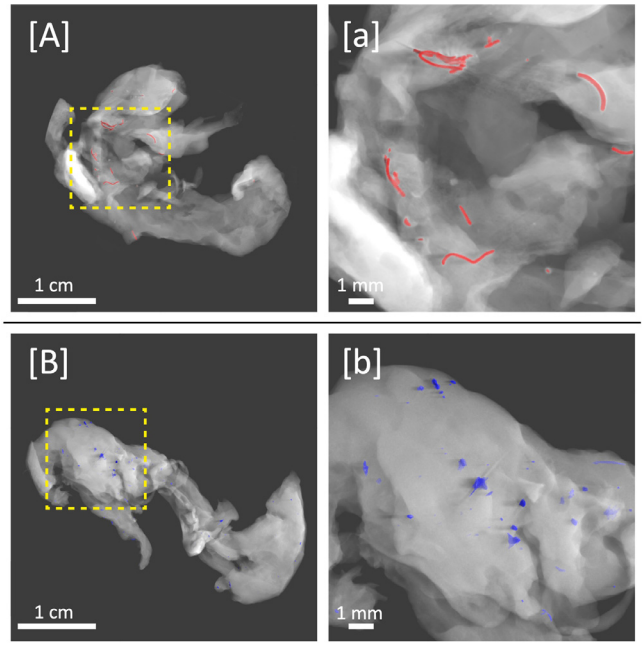

Fig. 3. [A] and [B] show the results of the µCTs of the soft tissue samples. The 3-D rendering of the two tissue specimens is shown on the left. [A] and the zoom in [a] show peri–implant soft tissue from a CFR-PEEK plate: colored in red, particles and longer fibers of different sizes and configurations are shown in the tissue indicated in gray. [B] and the zoom in [b] show peri–implant soft tissue from a titanium plate: colored in blue, particles of different sizes can be seen in the tissue shown in gray. (For interpretation of the references to color in this figure legend, the reader is referred to the web version of this article.)

3. Results

3.1. µCT of peri–implant soft tissue

The µCT of the soft tissue shows entrapped particles of different shape, configuration and size. In the peri–implant soft tissue over CFR-PEEK plates larger fiber and wire fragments as well as smaller roundish particles were found, whereas in the peri–implant soft tissue over titanium plates only smaller foreign bodies could be detected. Fig. 3 shows two examples of soft tissue samples with enclosed foreign bodies.

3.2. Histology

Soft tissue removal yielded samples with different volumes and varying tissue density, which sometimes made it difficult to cut them with a standard paraffin microtome. Routine H&E-stained sections (Fig. 4) showed dark, irregularly distributed particles in the tissue samples neighbouring the two types of implants. Particles varied in size and shape. The semi-quantitative assessment of the immunohistochemically labelled sections revealed that a wide range of different macrophages is present in the connective tissue next to implants. Labelling intensity of the tissue matrix was not considered, instead only the number of positive cells was recorded for each antibody. Since the distribution of positive cells per section was very inhomogeneous, the limitation to a single field of view was not suitable for this type of assessment. Thus, the entire section had to be evaluated.

In the sections immunolabelled with an antibody against CD68, a universal macrophage marker, more than 10 cells were positive in 6 CFR-PEEK and 7 titanium samples. The other 2 and 1 samples showed at least 2–9 positive cells (Figs. 5 and 6). The statistical analysis showed no significant difference between CFR-PEEK and titanium ($p = 0.535$).

When assessing the results for CD163, a marker expressed on M2 macrophages, 2 of the 8 tissue samples from CFR-PEEK plates had more than 10 positive cells, one sample had 2–9 positive cells, while in 3 one cell was detected positive. The remaining 2 samples were negative. In the soft tissue over titanium plates, 2–9 cells are positive in 4 samples and 1 cell in 1 sample; 3 samples were negative (Figs. 5 and 6). The statistical evaluation showed no significant difference between CFR-PEEK and titanium ($p = 0.702$).

After labelling with 25F9, an antibody recognizing mature, tissue-fixed macrophages, 6 samples from the soft tissue of CFR-PEEK plates showed 2–9 positive cells and 2 samples were negative. In the soft tissue from titanium plates, 2–9 cells were positive in one sample, 1 cell in 2 samples, and 5 samples were negative (Figs. 5 and 6). The statistical analysis of the semiquantitative evaluation showed significantly more positive cells in the soft-tissue over CFR-PEEK than over titanium ($p = 0.038$).

When labelling with an antibody against Calprotectin (MRP8/14), a marker constitutively expressed in neutrophils and monocytes (both cell types also may express CD68 and phagocytose extracellular material), all samples of CFR-PEEK plates showed more than 10 positive cells. In the soft tissue of titanium plates, more than 10 cells are positive in 4 samples, 2–9 cells are positive in 3 samples and 1 cell was positive in 1 sample (Figs. 5 and 6). The statistical analysis of the semiquantitative evaluation showed significantly more positive cells in the soft-tissue over CFR-PEEK than over titanium ($p = 0.027$).

It should be noted that CD68 is a common marker for all types of macrophages occurring at different stages of inflammation while the other three antibodies recognize cells (with elevated macrophage activity or not) which are indicative of early, intermediate or late stages of inflammation.

3.3. Infrared microscopy (FTIR)

FTIR microscopy was used in the investigation of particles with regard to their material composition, in which it was confirmed that the particles in the soft tissue over CFR-PEEK plates consist of PEEK and carbon fiber. Fig. 7 shows spectra of an identified PEEK particle (red spectrum; with some residues of the PMMA resin) and carbon fiber (black) in the sample as well as reference spectra of PEEK (blue) and PMMA (green). Spectra obtained from the sample are showing increased absorbance towards lower wavenumber due to an optical effect of carbon in the carbon fibers (see black spectrum).

3.4. HR-CT-scans of paraffin-embedded soft tissue and plates

The HR-CT-scans of the CFR-PEEK plates show the different orientation of the carbon fibers as well as the high density (Fig. 8[A]). Furthermore, the apparently randomly embedded tantalum wires can be seen in the HR-CT-scans of the CFR-PEEK plates (Fig. 8[B]). Moreover, it is remarkable that the tantalum wires are particularly dense around screw holes (Fig. 8[B] marked with asterisk) and that some of the tantalum wires are detached from the bond and protrude into the screw hole (Fig. 8[B] marked with arrow).

When we further analyzed the soft tissue samples with HR-CT-scans (see Fig. 9), we could detect clear particle inclusions, which are assigned to different materials based on their X-ray attenuation values compared to similarly sized reference metal samples embedded in paraffin and measured under identical conditions. The

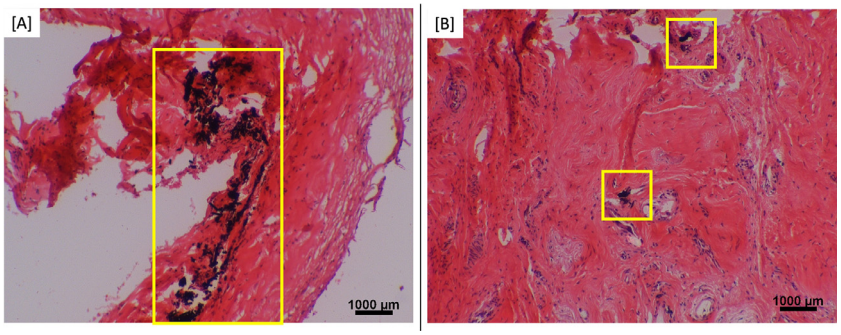

Fig. 4. HE stained sections of soft tissue specimens. [A] shows soft tissue from a CFR-PEEK plate. Framed in yellow, foreign bodies of different configuration and size are seen. [B] shows soft tissue from a titanium plate. Again, foreign particles are shown framed in yellow. (For interpretation of the references to color in this figure legend, the reader is referred to the web version of this article.)

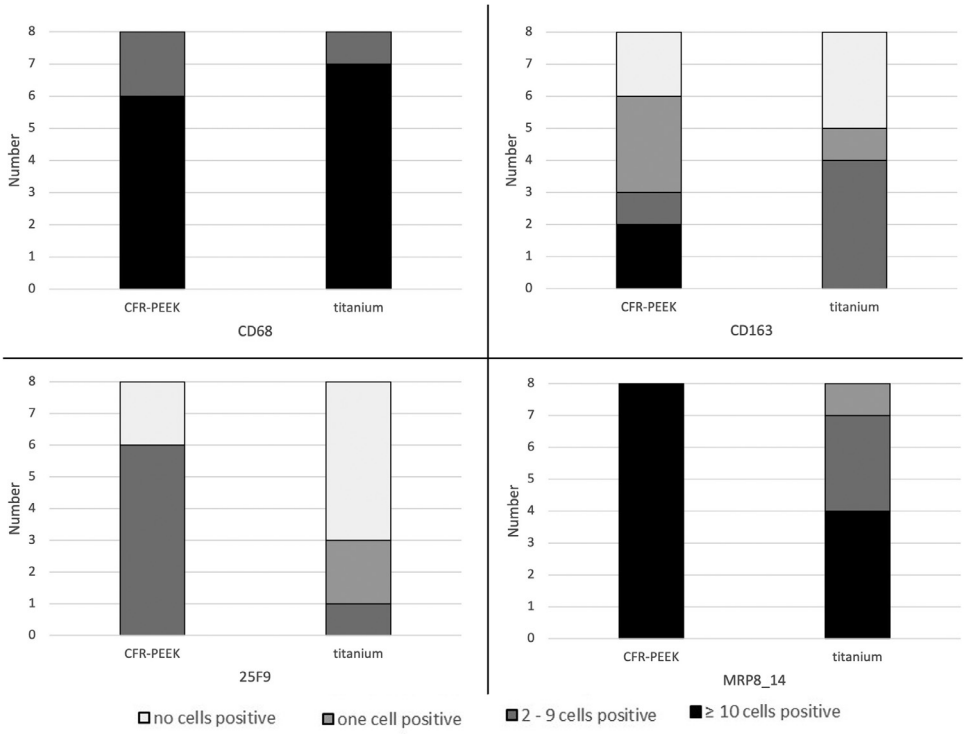

Fig. 5. Graphic visualization of the results of the semi-quantitative evaluation of immunohistochemical slides. Samples are plotted on the *Y*-axis in each case; a black bar indicates ≥ 10 positive cells, a dark gray bar represents 2–9 positive cells, a light gray bar means 1 positive cell, and a white bar indicates no positive cells. The left column shows the CFR-PEEK samples and the right column the titanium samples. (For interpretation of the references to color in this figure legend, the reader is referred to the web version of this article.)

most attenuating metal is tantalum, followed by titanium, while the least radio dense materials that could be identified in the sample are particles of PEEK and carbon fibers.

3.5. Scanning electron microscopy (SEM) and energy dispersive X-ray analysis (EDX)

On the surface of the explanted CFR-PEEK plates, which appears rough in SEM, larger pits and exposed carbon fibers (Ø 3 µm approx.) can be seen, some of which show fractures (Fig. 10[B]). A closer look at the screw holes in the SEM of explanted CFR-PEEK plates (Fig. 10[C]) reveals individual tantalum wires (Ø 50 µm approx.), that are partially detached from the composite and lie freely in the hole (Fig. 10[C]). It can be seen that these are heavily deformed and twisted in some places (Fig. 10[C] and [D]). Elemental analysis by EDX shows that the deformed areas of the wires have a higher titanium-aluminum-vanadium content than the round tantalum wires (Fig. 10[E]). As typical for explanted implant materials some small residua from body fluids and small tissue fragments were found on surfaces and in cavities (see Fig. 12 & Suppl. Fig. 1).

Interestingly, SEM images of the new CFR-PEEK plates revealed exposed tantalum wires and carbon fibers on the surface in some of the pre-shaped holes (Fig. 11[A] and [B]). All areas were assigned to the respective materials by EDX element analysis. Furthermore, there are exposed carbon fibers, only some of which are sheathed by PEEK. The exposed tantalum wires already show scratches and notches even in the unused state (see Figs. 10 & 11).

On the surface of the explanted PHILOS® some scratches (Fig. 12) as well as some small areas with biological residua are visible. All inspected pre-milled threads in screw holes were intact and did not show damages.

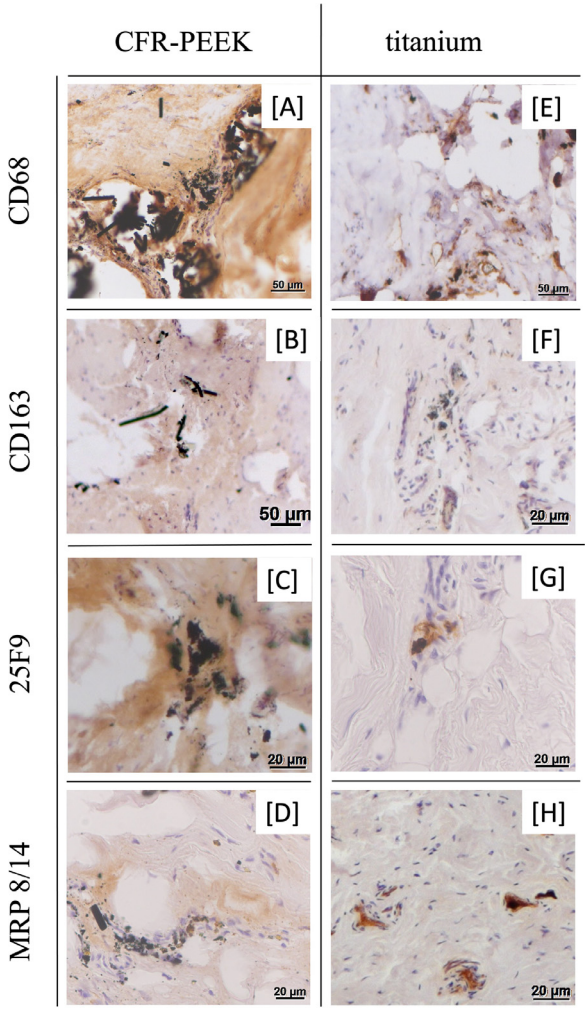

Fig. 6. Images of the different immunohistochemical stains (CD68, CD163, mature, tissue fixed macrophage antigen (25F9) and calprotectin (MRP8/14)). The left column ([A] - [D]) shows samples from peri–implant soft tissue of CFR-PEEK plates and the right column ([E] - [H]) shows samples from titanium plates. The positive cells are brown, they are found especially around small particles. (For interpretation of the references to color in this figure legend, the reader is referred to the web version of this article.)

3.6. Roughness measurement of surfaces by white light profilometry

The roughness measured for the explanted CFR-PEEK plate examined revealed an Ra of 1.42 ± 0.25 µm, whereas the used titanium plate had an Ra of 0.51 ± 0.21 µm ($p = 0.022$). The graphical representations of the results are shown in the Suppl. Fig. 2. However, it should be mentioned that the explanted plates still contained biological residues from the time in vivo.

4. Discussion

The purpose of this study was to evaluate the inflammatory tissue response to osteosynthesis plates made of CFR-PEEK and titanium, which also have two different locking mechanisms for the screw heads. Different particles could be seen in histological examination and CT-scans in peri-implant soft tissue neighboring explanted CFR-PEEK and titanium plates. However, significantly more inflammatory tissue response in soft tissue over explanted CFR-PEEK plates, compared to soft tissue over explanted titanium plates could be demonstrated in the immunohistochemical examination. Using infrared microscopy, it was possible to prove that the particles in the soft tissue over CFR-PEEK plates consisted of carbon fibers and PEEK fragments from the plates, as they had the same spectrum. Furthermore, it could be shown that they were not entrained particles such as stainless steel from instruments used for im- and explantation. Since the question arose as to where these particles came from, the plates were examined in more detail using SEM, EDX and HR-CT. The roughness measurements of Ra values on both plate materials showed significantly rougher surfaces of the CFR-PEEK plates compared to the titanium plates. Furthermore, fragmented carbon fibers could be detected on the surface of the CFR-PEEK plates, which according to their size of only about 3 µm could be ingested by macrophages while larger fragments are too big to fit into a single cell. In addition, the screw holes of the plates showed exposed, partially protruding and partially crushed tantalum filaments, which presumably came off when the thread was screwed in to provide angular stable fixation since the degree of TiAlV of the tantalum wire corresponded with the degree of deformation.

Another possible source of particle release could be movement in the implant-bone or plate-screw interface during the time in situ. Preliminary work on load to failure and movement in the bone-implant interface comparing the titanium alloy PHILOS® and PEEK plates for the proximal humerus showed that the polymer implants had a lower load to failure and allowed significantly more

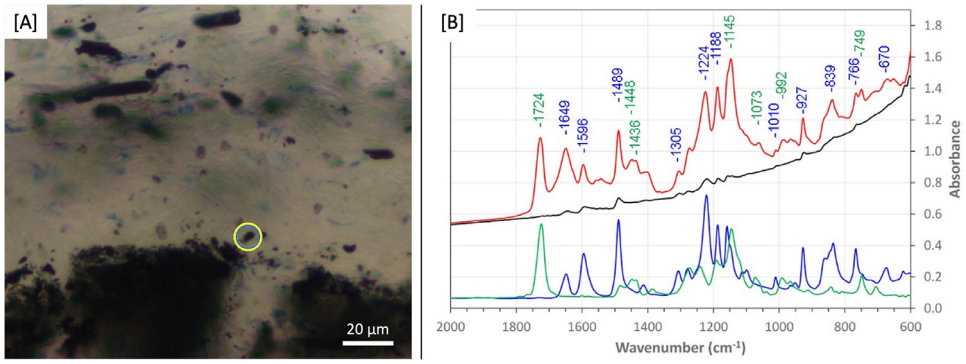

Fig. 7. FTIR microscopy of peri–implant tissue embedded in PMMA with Giemsa-eosin surface stain: In the optical image [A], the analyzed area appears roughened compared to the original surface. The foreign particle is marked with a yellow ring and the corresponding FTIR spectrum is shown in [B] as a red line. Comparison with reference spectra of PEEK (blue line), carbon fibers (black line) and PMMA (green line) identifies the foreign particle as a composite of PEEK and carbon fibers with residues of PMMA coming from the resin. (For interpretation of the references to color in this figure legend, the reader is referred to the web version of this article.)

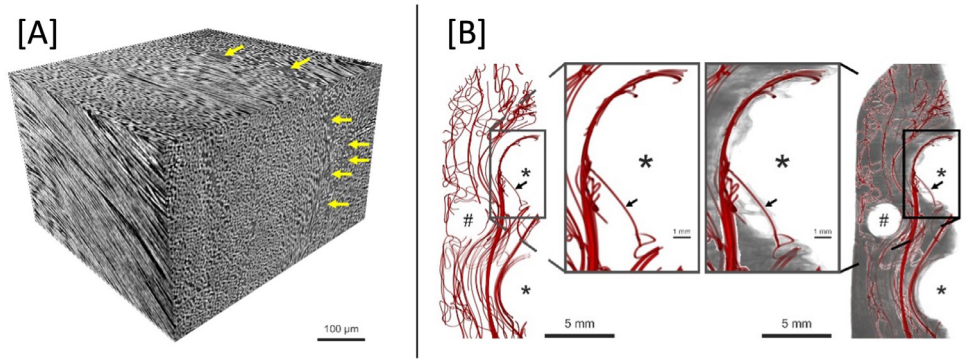

Fig. 8. HR-CT-scans of explanted CFR-PEEK plates. [A] shows a 3D rendering of the densely packed carbon fibers in the PEEK matrix. The orientation and the density of fibers (yellow arrows) differ in various regions. The reconstruction of the network of red tantalum wires in [B] illustrates the locally different number of wires. Asterisks mark the screw holes, arrows mark tantalum wires that have been released from the composite, # marks a thread hole on the outer rim of the plate. (For interpretation of the references to color in this figure legend, the reader is referred to the web version of this article.)

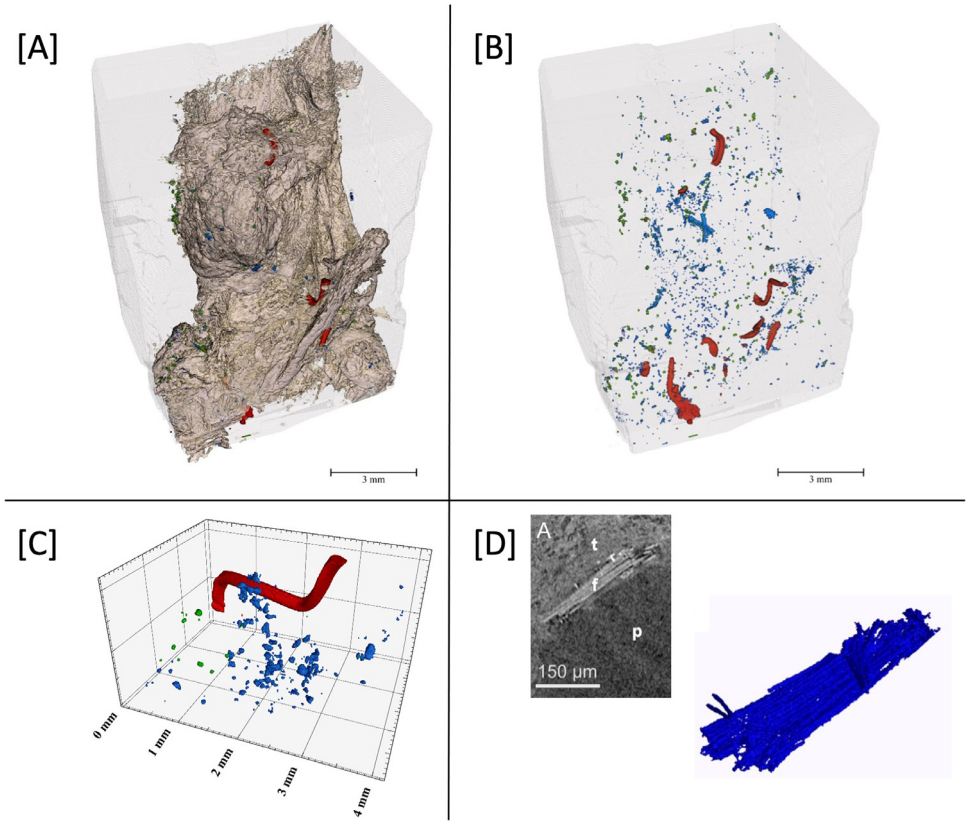

Fig. 9. High resolution CT-scans of Paraffin-embedded soft tissue. 3D rendering of the paraffin block with tissue (brownish) and debris in different colors depending on their attenuation are shown in [A] and only the inclusions and the paraffin (the tissue was made transparent) in [B]. The foreign objects were color-coded: red for the highest absorbing metals (indicative for tantalum wires), green for medium absorbing (indicative for titanium, if present) and blue for lowest absorbing material such as PEEK and carbon fibers. [C] and [D] show foreign objects in larger magnification. Several chunks of broken-off carbon fiber bundles are clearly visualized in the tissue by HR-CT. (For interpretation of the references to color in this figure legend, the reader is referred to the web version of this article.)

movement in the bone-implant interface [18,19]. This could also explain the higher concentration of foreign bodies in the soft tissue over CFR-PEEK plates compared to the titanium group in this study. However, both biomechanical studies only model the very first time the plates are in situ, when the fracture gaps are not filled with newly formed tissue yet. Furthermore, the biomechanical testing does not simulate everyday conditions [18,19].

At this point it must be emphasized that osteosynthesis plates, in contrast to e.g. arthroplasty, are in many cases removed again after a certain period of time [20]. Accordingly, the authors of this paper assume that the particles are predominantly released during implantation and to a lesser extent during the time in situ. This is a different mechanism of particle formation compared to the generation of wear particles in arthroplasties, where they are usually formed by the load and (micro-)movement during the time in situ and only in smaller proportions during implantation [21,22].

This study has used a variety of methods to examine the plates and peri–implant soft tissue. It turned out that due to the different size and materials of the particles, one method alone is not sufficient. Particularly histology and CT had complementary effects: Larger foreign particles (> 20 µm) are often simply torn out when the histological sections are cut, whereas the resolution of the CT reaches its limits with the smallest particles, which are still seen in histology. Furthermore, the three-dimensional reconstruc-

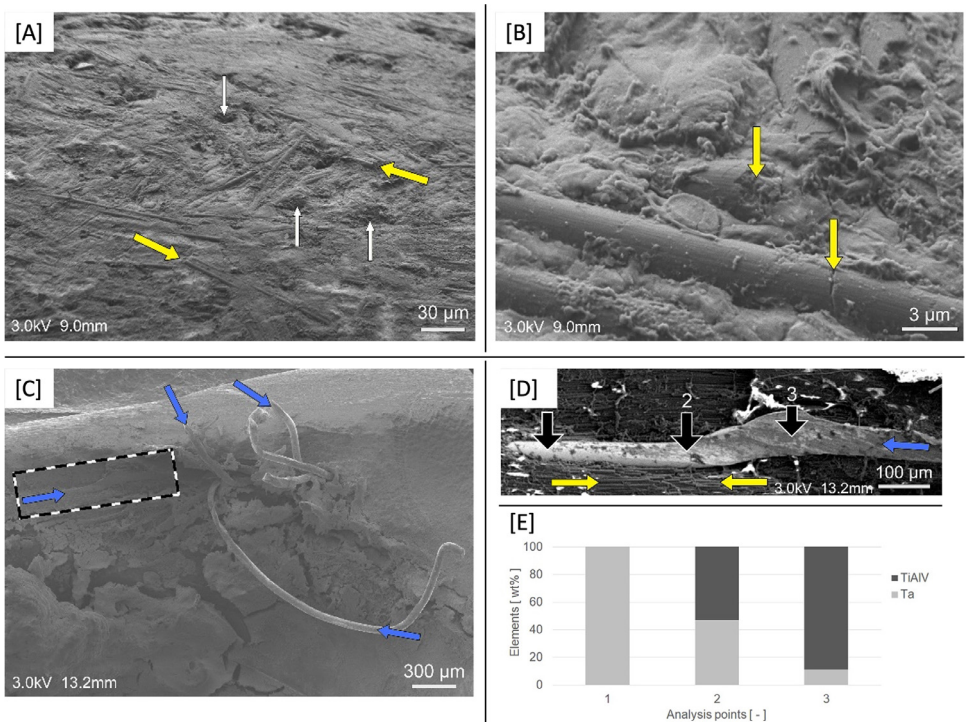

Fig. 10. Explanted CFR-PEEK plate in SEM: at lower magnification in [A], the surface appears quite rough with frequent deeper pits (white arrows). Several carbon fibers (yellow arrows) are exposed to the tissue, some are covered with PEEK. At higher magnification in [B] cracks and fractures of carbon fibers were found. In a used locking head screw hole of an explanted CFR-PEEK plate [C], the protruding, twisted and bent tantalum wires marked with blue arrows were conspicuous. In the closer view, marked with a rectangular shape and shown in [D], a tantalum wire (blue arrow) can be seen deep in the PEEK plate next to carbon fibers (yellow arrows). The wire appears partially not circular and deformed. The dark grey regions on the light grey areas of the wire correspond to the degree of deformation as well as the content of titanium-aluminum-vanadium (TiAlV) relative to tantalum (Ta) as determined by EDX as shown in the diagram [E]. The black arrows in [D] correspond to the bars of the diagram in [E]. The detailed EDX spectra from the three analysis points marked in [D] and [E] are represented in suppl. Fig. 3. (For interpretation of the references to color in this figure legend, the reader is referred to the web version of this article.)

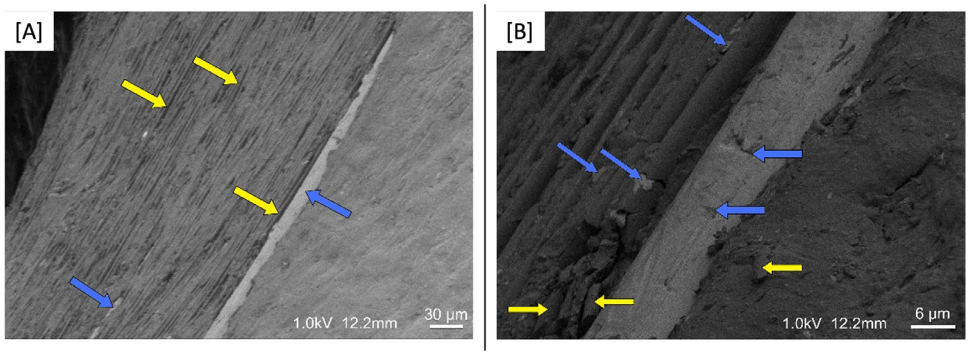

Fig. 11. SEM images of a screw hole in a new CFR-PEEK plate. In the overview image [A], the light grey tantalum wires (blue arrows) can be seen on the surface of the screw hole. The element tantalum was identified at each of these locations by EDX. Several carbon fibers (yellow arrows) were also exposed on the surface, and several others were covered with PEEK. In magnification image [B], several small fragments of PEEK, carbon fibers (yellow arrows), or tantalum (small blue arrows) can be detected. The prominent light gray tantalum wire shows scratches and cavities on the surface, which are marked with larger blue arrows. The detailed EDX spectra from the prominent light gray tantalum wire is shown in Suppl. Fig. 4. (For interpretation of the references to color in this figure legend, the reader is referred to the web version of this article.)

tion of the CT-scans of the intact samples enables the spatial assessment of the particles in the soft tissue and allows an accurate morphological description of the larger foreign bodies. However, it should be noted that due to the similar radiodensity of PEEK, carbon fibers and the surrounding soft tissue, it is not possible to visualize foreign bodies from these materials in the µCT of the peri–implant soft tissue. Only the tantalum wires and titanium particles are visualized here. HR-CT of the paraffin-embedded samples also reaches its limits the smaller these particles become, so it can be assumed that information is also lost here, and the true extent of the PEEK and carbon fiber particle load cannot be shown using CT. Especially with regard to the smallest particles, a thorough assessment in this study is only possible with histology. A precise description regarding the material composition was provided by FTIR, where the exact material composition of individual foreign bodies could be determined in the histological section.

To the authors' knowledge, this is the first study that has examined human soft tissue over osteosynthesis plates of different materials in more detail and with such a variety of different methods. As one result, the study demonstrated that the inflammatory tissue response is significantly stronger over CFR-PEEK plates, com-

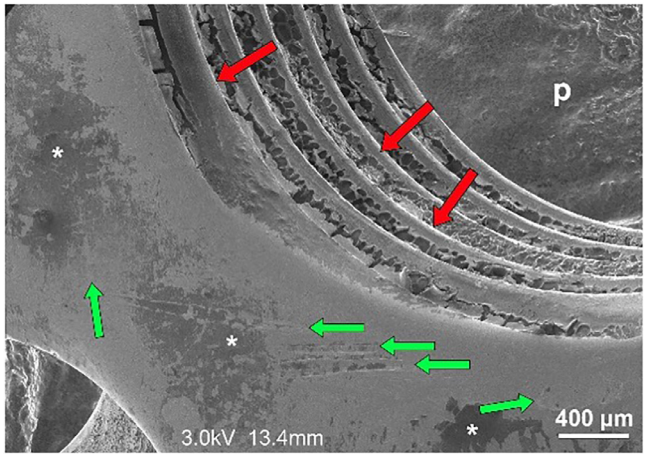

Fig. 12. SEM image from the surface and a used screw hole of an explanted titanium plate. On the surface some smaller scratches and marks are visible (small light green arrows) and the thread is intact (large red arrows) covered with biological residua. Even on the smooth surface residua could be found as darker regions (*). p labels the conductive preparation material. (For interpretation of the references to color in this figure legend, the reader is referred to the web version of this article.)

pared to soft tissue over titanium alloy plates. These results are supported by a study that found similar tissue reactions and particles in the overlying synovium after explantation of PEEK hip prostheses [23].

Interestingly, the inflammatory cells in this study are mainly found around collections of small and minute particles. The large clusters of foreign material show fewer inflammatory cells in their vicinity. The authors attribute this to the fact that the smallest particles can be internalized by macrophages, but the large fragments are indigestible for them. This assumption is supported by the results of a 2016 publication that investigated which size of titanium particles stimulates macrophage polarization. It turned out that not nanoparticles (< 100 nm) but microparticles (< 5 µm) are the largest inducers of such reprogramming [24]. Nevertheless, the question remains what happens to the accumulations of larger particles. Furthermore, it remains unclear how the trapped particles are possibly digested and where the cells transport them. These results are contrary to findings made by Nieminen et al. who showed no relevant number of macrophages or particles in the surrounding tissue of pure PEEK plates, which were implanted in the subcutaneous tissue of sheep [25]. However, it should be noted that these plates were not fixed to the bone; accordingly, no screws were inserted into the plate bushings [25]. This fact supports the theory of the authors of this study that the fragments were released when the threads were screwed in. The results of Avery et al. on the other hand, support the results of this work [26]. They were able to show that when PEEK and titanium were implanted into mice, proinflammatory macrophages were activated around PEEK implants. They also conclude that a stronger inflammatory response is induced by PEEK than by titanium or titanium alloys [26].

The HR-CT-scans and the SEM of the plates showed fragmented carbon fibers with a size of about 3 µm on the rough surface of the new, unused plates as well as on the explanted plates made of CFR-PEEK on the one hand and partially exposed tantalum threads on the other hand. Since the plates had not yet been implanted, damage to the surface during surgery or implant removal could be ruled out. It can therefore be assumed that these originated from the manufacturing process. Due to the size of the carbon fiber fragments of approximately 3 µm, the particles can be ingested by macrophages [24]. Studies showed that titanium particles of this size stimulate the polarization of macrophages from the native M0 to the proinflammatory M1 phenotype [24,27] and therefore cause inflammation, which leads to proliferation of fibroblasts. This tissue proliferation, in turn, is suspected, among other factors, to cause movement restrictions in the affected joints [28]. Whether also carbon fragments and PEEK particles induce macrophage polarization has not yet been investigated. As infrared microscopy showed, the particles in the soft tissue also consist of PEEK, which comes from the plates, too. These particles are capable of inducing an inflammatory reaction as well. This was shown in a 2018 publication in which PEEK wear particles in rat knees triggered inflammation induced and maintained by CD8+ *T* cells [29].

Moreover, tantalum wires were detected in the screw bushings of the explanted plates, which had partially detached from the bond. The most likely reason here was cutting of the thread during insertion of the locking screws. In 2002, Langford et al. confirmed the results of a study conducted in 1998 by identifying production defects such as rough corners and protruding edges as well as damage presumably caused during the implantation process in the SEM analysis of maxillofacial titanium plates [30,31]. However, there was no increased corrosion or surface deterioration. Whether the damaged plates caused an increased inflammatory reaction or soft tissue hypertrophy was not evaluated [30]. Nevertheless, preliminary work showed that tantalum improves the cell adhesiveness of implant materials [32]. This is certainly advantageous, for example, when it comes to osseointegration of dental implants, but disadvantageous when it potentially causes soft tissue adhesions to osteosynthesis plates and thus movement limitations.

The challenges of the manufacturing process of orthopedic implants made of CFR-PEEK composites also become evident in a finite element analysis, in which was shown that the arrangement of the layers in relation to each other is decisive for the bending and torsional strength of the material [33]. It was also shown here that cracks cause the carbon fibers to detach from the PEEK [33].

In addition, it must be reflected whether the rough surface contributes to the adhesion of connective tissue and thus promotes an unwanted ingrowth into the surrounding soft tissue in the case of osteosynthesis plates. In previous work, it was shown that surface properties have an influence on cell adhesion [34]. Some studies have already been published on the optimal CFR-PEEK surface for osteointegrative implants, but there is a lack of studies dealing with surfaces that provoke as little cell adhesion as possible. Here, CFR-PEEK with its hydrophobicity already seems to have good prerequisites [9], but nevertheless adjustments still seem to be necessary. It remains to be proven whether smoother, polished CFR-PEEK plates result in less adhesion to surrounding soft tissue.

It should be emphasized that both plate systems have advantages and disadvantages. The CFR-PEEK plates used can be fixed polyaxially in the bone, allowing the surgeon to place the screws in bone with best quality. In addition, the radioluminescence of the polymer plates enables better control of the reduction in X-rays. This is counterbalanced by the higher particle load and significantly more pronounced inflammatory reaction to the particles in the surrounding soft tissue. The present study does not allow a direct distinction as to whether the material used or the number of particles produced by the different implants is the main factor for the observed inflammatory reaction. The titanium plates, on the other hand, can only be fixed monoaxially, but offer the possibility of screw tip augmentation, which increases the bone-implant interface, resulting in better screw retention in bone with poor quality. In addition, fewer particles were found in the soft tissue over titanium plates, which also induced significantly less inflammation. Which implant the surgeon ultimately chooses therefore remains a case-by-case decision.

However, based on the results of this study, the authors tend to advise their patients with CFR-PEEK plates to have the implant and adjoining scar tissue removed after fracture healing is complete.

Regarding the limitations of this study, it must be mentioned that in each experimental group only the implants and implant materials of one manufacturer were evaluated. Furthermore, regarding angular stability, it must be emphasized that the titanium implant evaluated is a monoaxial system and the CFR-PEEK plates are polyaxial due to the screws cutting the threads into the bushings of the plate. However, there are also systems in which the plate thread is already pre-milled, so that there is certainly less abrasion in the patient‘s body and also less damage to the plate.

In conclusion, the presented work shows that after explantation of locking plates made of CFR-PEEK and titanium on the proximal humerus, distinctly more particles are present in the soft tissue over CFR-PEEK than in that over titanium plates. These particles also induce a stronger inflammatory tissue reaction, which could be detected by immunohistochemistry. As a possible explanation, the authors assume that the particles were formed when the titanium screws were screwed into the CFR-PEEK plates. This hypothesis is supported by the SEM and HR-CT results, which showed that carbon fibers and tantalum wires were partially detached from the plate composite.

Abbreviations

CFR-PEEK = carbonfiber reinforced Polyetheretherketone
CT = computer tomography
HR-CT = High resolution computer tomography
FTIR = Fourier transform infrared spectroscopy
SEM = Scanning electron Microscope
EDX = Energy Dispersive X-ray analysis

The raw/processed data required to reproduce these findings cannot be shared at this time due to legal or ethical reasons.

Declaration of competing interest

The authors declare that they have no known competing financial interests or personal relationships that could have appeared to influence the work reported in this paper.

CRediT authorship contribution statement

E Fleischhacker: Data curation, Formal analysis, Funding acquisition, Investigation, Methodology, Project administration, Supervision, Visualization, Writing – original draft, Writing – review & editing, Resources. **CM Sprecher:** Formal analysis, Investigation, Methodology, Software, Validation, Visualization, Writing – original draft, Writing – review & editing. **S Milz:** Data curation, Formal analysis, Investigation, Visualization, Writing – original draft, Writing – review & editing. **MM Saller:** Data curation, Formal analysis, Investigation, Software, Validation, Visualization, Writing – original draft. **R Wirz:** Data curation, Software, Validation, Visualization, Writing – original draft. **R Zboray:** Data curation, Investigation, Software, Validation, Visualization, Writing – original draft, Writing – review & editing. **A Parrilli:** Data curation, Formal analysis, Software, Visualization, Writing – original draft, Writing – review & editing. **J Gleich:** Data curation, Investigation, Validation. **G Siebenbürger:** Data curation, Formal analysis, Resources. **W Böcker:** Resources, Supervision. **B Ockert:** Conceptualization, Supervision. **T Helfen:** Conceptualization, Supervision.

Supplementary materials

Supplementary material associated with this article can be found, in the online version, at doi:10.1016/j.actbio.2024.04.023.

References

[1] L. Howard, R. Berdusco, F. Momoli, J. Pollock, A. Liew, S. Papp, K.A. Lalonde, W. Gofton, S. Ruggiero, P. Lapner, Open reduction internal fixation vs non-operative management in proximal humerus fractures: a prospective, randomized controlled trial protocol, BMC Musculoskelet. Disord. 19 (1) (2018) 299.
[2] M. Kettler, P. Biberthaler, V. Braunstein, C. Zeiler, M. Kroetz, W. Mutschler, [Treatment of proximal humeral fractures with the PHILOS angular stable plate. Presentation of 225 cases of dislocated fractures], Unfallchirurg 109 (12) (2006) 1032–1040.
[3] B. Ockert, G. Siebenburger, M. Kettler, V. Braunstein, W. Mutschler, Long-term functional outcomes (median 10 years) after locked plating for displaced fractures of the proximal humerus, J. Shoulder Elbow Surg. 23 (8) (2014) 1223–1231.
[4] Thomsen, M. and P. Thomas, [Compatibility and allergies of osteosynthesis materials]. Unfallchirurg, 2017. 120(2): p. 116–121.
[5] G. Voggenreiter, S. Leiting, H. Brauer, P. Leiting, M. Majetschak, M. Bardenheuer, U. Obertacke, Immuno-inflammatory tissue reaction to stainless-steel and titanium plates used for internal fixation of long bones, Biomaterials 24 (2) (2003) 247–254.
[6] X. He, F.X. Reichl, S. Milz, B. Michalke, X. Wu, C.M. Sprecher, Y. Yang, M. Gahlert, S. Rohling, H. Kniha, R. Hickel, C. Hogg, Titanium and zirconium release from titanium- and zirconia implants in mini pig maxillae and their toxicity in vitro, Dent. Mater. 36 (3) (2020) 402–412.
[7] S.M. Kurtz, J.N. Devine, PEEK biomaterials in trauma, orthopedic, and spinal implants, Biomaterials 28 (32) (2007) 4845–4869.
[8] C.S. Li, C. Vannabouathong, S. Sprague, M. Bhandari, The use of carbon-fiber-reinforced (CFR) PEEK material in orthopedic implants: a systematic review, Clin. Med. Insights Arthritis Musculoskelet. Disord. 8 (2015) 33–45.
[9] R. Ding, T. Chen, Q. Xu, R. Wei, B. Feng, J. Weng, K. Duan, J. Wang, K. Zhang, X. Zhang, Mixed modification of the surface microstructure and chemical state of polyetheretherketone to improve its antimicrobial activity, hydrophilicity, cell adhesion, and bone integration, ACS Biomater. Sci. Eng. 6 (2) (2020) 842–851.
[10] J. Caballe-Serrano, V. Chappuis, A. Monje, D. Buser, D.D. Bosshardt, Soft tissue response to dental implant closure caps made of either polyetheretherketone (PEEK) or titanium, Clin. Oral Implants Res. 30 (8) (2019) 808–816.
[11] D. Togawa, T.W. Bauer, J.W. Brantigan, G.L. Lowery, Bone graft incorporation in radiographically successful human intervertebral body fusion cages, Spine (Phila Pa 1976) 26 (24) (2001) 2744–2750.
[12] T. Tullberg, Failure of a carbon fiber implant. A case report, Spine (Phila Pa 1976) 23 (16) (1998) 1804–1806.
[13] A. Merolli, L. Rocchi, M. De Spirito, F. Federico, A. Morini, L. Mingarelli, F. Fanfani, Debris of carbon-fibers originated from a CFRP (pEEK) wrist-plate triggered a destruent synovitis in human, J. Mater. Sci. Mater.. Med 27 (3) (2016) 50.
[14] D. Paganin, S.C. Mayo, T.E. Gureyev, P.R. Miller, S.W. Wilkins, Simultaneous phase and amplitude extraction from a single defocused image of a homogeneous object, J. Microsc. 206 (Pt 1) (2002) 33–40.
[15] R. Zboray, Optimizing and applying high-resolution, in-line laboratory phase–contrast X-ray imaging for low-density material samples, J. Microsc. 282 (2) (2021) 123–135.
[16] L.A. Feldkamp, D.L. Kress JW, Practical cone-beam algorithm, J. Opt. Soc. Am. 1 (1984) 612–619.
[17] J.S. Hayes, U. Seidenglanz, A.I. Pearce, S.G. Pearce, C.W. Archer, R.G. Richards, Surface polishing positively influences ease of plate and screw removal, Eur. Cell Mater. 19 (2010) 117–126.
[18] J.C. Katthagen, M. Schwarze, M. Warnhoff, C. Voigt, C. Hurschler, H. Lill, Influence of plate material and screw design on stiffness and ultimate load of locked plating in osteoporotic proximal humeral fractures, Injury 47 (3) (2016) 617–624.
[19] B. Schliemann, R. Seifert, C. Theisen, D. Gehweiler, D. Wahnert, M. Schulze, M.J. Raschke, A. Weimann, PEEK versus titanium locking plates for proximal humerus fracture fixation: a comparative biomechanical study in two- and three-part fractures, Arch. Orthop. Trauma Surg. 137 (1) (2017) 63–71.
[20] M.L. Busam, R.J. Esther, W.T. Obremskey, Hardware removal: indications and expectations, J. Am. Acad. Orthop. Surg. 14 (2) (2006) 113–120.
[21] J. Jamari, M.I. Ammarullah, G. Santoso, S. Sugiharto, T. Supriyono, A.T. Prakoso, H. Basri, E. van der Heide, Computational contact pressure prediction of CoCrMo, SS 316L and Ti6Al4V femoral head against UHMWPE acetabular cup under gait cycle, J. Funct. Biomater. 13 (2) (2022).
[22] A.A. Stratton-Powell, S. Williams, J.L. Tipper, A.C. Redmond, C.L. Brockett, Isolation and characterisation of wear debris surrounding failed total ankle replacements, Acta Biomater. 159 (2023) 410–422.
[23] A.M. Latif, A. Mehats, M. Elcocks, N. Rushton, R.E. Field, E. Jones, Pre-clinical studies to validate the MITCH PCR Cup: a flexible and anatomically shaped acetabular component with novel bearing characteristics, J. Mater. Sci. Mater. Med. 19 (4) (2008) 1729–1736.
[24] A.D. Schoenenberger, A. Schipanski, V. Malheiro, M. Kucki, J.G. Snedeker, P. Wick, K. Maniura-Weber, Macrophage polarization by titanium dioxide (TiO2) particles: size matters, ACS Biomater. Sci. Eng. 2 (6) (2016) 908–919.
[25] T. Nieminen, I. Kallela, E. Wuolijoki, H. Kainulainen, I. Hiidenheimo, I. Rantala, Amorphous and crystalline polyetheretherketone: mechanical properties and tissue reactions during a 3-year follow-up, J. Biomed. Mater. Res. A 84 (2) (2008) 377–383.

[26] D. Avery, L. Morandini, N. Celt, L. Bergey, J. Simmons, R.K. Martin, H.J. Donahue, R. Olivares-Navarrete, Immune cell response to orthopedic and craniofacial biomaterials depends on biomaterial composition, Acta Biomater. 161 (2023) 285–297.
[27] J.K. Antonios, Z. Yao, C. Li, A.J. Rao, S.B. Goodman, Macrophage polarization in response to wear particles in vitro, Cell Mol. Immunol. 10 (6) (2013) 471–482.
[28] Tauro, J.A., R. L., The shoulder. AANA Advanced Arthroscopy Series, ed. R.K.N. Ryu 2010: Elsevier. 10.
[29] Z. Du, S. Wang, B. Yue, Y. Wang, Y. Wang, Effects of wear particles of polyether-ether-ketone and cobalt-chromium-molybdenum on CD4- and CD8-T-cell responses, Oncotarget 9 (13) (2018) 11197–11208.
[30] R.J. Langford, J.W. Frame, Surface analysis of titanium maxillofacial plates and screws retrieved from patients, Int. J. Oral Maxillofac. Surg. 31 (5) (2002) 511–518.
[31] M.S. Ray, I.R. Matthew, J.W. Frame, Metallic fragments on the surface of miniplates and screws before insertion, Br. J. Oral Maxillofac. Surg. 37 (1) (1999) 14–18.
[32] S. Mei, L. Yang, Y. Pan, D. Wang, X. Wang, T. Tang, J. Wei, Influences of tantalum pentoxide and surface coarsening on surface roughness, hydrophilicity, surface energy, protein adsorption and cell responses to PEEK based biocomposite, Colloids Surf. B Biointerfaces 174 (2019) 207–215.
[33] E.A. Gallagher, S. Lamoriniere, P. McGarry, Finite element investigation into the use of carbon fibre reinforced PEEK laminated composites for distal radius fracture fixation implants, Med. Eng. Phys. 67 (2019) 22–32.
[34] B.J. Yoon, F. Xavier, B.R. Walker, S. Grinberg, F.P. Cammisa, C. Abjornson, Optimizing surface characteristics for cell adhesion and proliferation on titanium plasma spray coatings on polyetheretherketone, Spine J. 16 (10) (2016) 1238–1243.